

## Original Article

# <sup>19</sup>F NMR Study on the Complex of Fluorinated Vitamin D Derivatives with Vitamin D Receptor: Elucidation of the Conformation of Vitamin D Ligands Accommodated in the Receptor

Daisuke Morizono

Graduate School of Medical and Dental Sciences, Institute of Biomaterials and Bioengineering, Tokyo Medical and Dental University

Nuclear receptors mediate allosteric communications where ligand binding initiates a cascade of signal transduction. The interaction of vitamin D with vitamin D receptor (VDR) was investigated by <sup>19</sup>F NMR spectroscopy of the complexes of three fluorinated vitamin D derivatives with the full-length rat VDR-LBD. In the <sup>19</sup>F NMR spectra of the VDR-ligand complexes, the A-ring of 4,4-difluoro-1,25(OH)<sub>2</sub>D<sub>3</sub> was revealed to adopt β-conformation in the VDR in solution, and the spectra were shown to be dependent on the dissociation constant. While the complex of 4,4-difluoro-1,25(OH)<sub>2</sub>D<sub>3</sub> with VDR exhibited a clear distinguishable <sup>19</sup>F NMR spectrum, those of <sup>19</sup>F-1,25(OH)<sub>2</sub>D<sub>3</sub> stereoisomers, which have 10-fold higher VDR affinity than 4,4-difluoro-1,25(OH)<sub>2</sub>D<sub>3</sub>, did not. The solid-phase NMR technique was useful for <sup>19</sup>F-1,25(OH)<sub>2</sub>D<sub>3</sub> stereoisomers. The fluorinated vitamin D derivatives showed marked changes in the chemical shift (Δ4–19.7 ppm) upon VDR-complex formation, and the *ab initio* MO method suggested that van der Waals interactions play a major role in the complex formation

**Key words:** <sup>19</sup>F NMR; vitamin D receptor; fluorinated vitamin D; *ab initio* MO; van der Waals interactions

## Introduction

Nuclear receptors (NRs)<sup>1-3</sup> are transcription factors whose functions are regulated by binding of a specific cognate ligand. Ligand binding changes the conformation of the ligand-binding domain (LBD) of NRs, and this triggers allosteric communication mediated by NRs<sup>4-7</sup>. The functions of the vitamin D receptor (VDR, NR111) are regulated by the active vitamin D metabolite, 1,25(OH)<sub>2</sub>D<sub>3</sub> (1). Extensive X-ray crystallographic studies have provided a great deal of information about the functions of NRs in relation to their structure<sup>8-14</sup>, particularly the mechanism of ligand-regulated NR activation. Since the crystal structure of the human VDR-LBD (Δ165–215) was first clarified in 2000<sup>14</sup>, the X-ray crystal structures of the human and rat VDR-LBD complex with more than 20 vitamin D derivatives have been filed in the Protein Data Bank (PDB)<sup>15-19</sup>. All these vitamin D ligands are anchored in the VDR ligand-binding pocket (LBP), forming three pairs of hydrogen bonds at their three hydroxyl groups, with some exceptions<sup>17</sup>, where an ordered water molecule included in the LBP substitutes the role of the hydroxyl group. Thus, correct positioning of these hydroxyl groups is important in order for 1,25(OH)<sub>2</sub>D<sub>3</sub> to exhibit its functions. All the vitamin D ligands in the VDR complexes adopt very similar conformations at the A-ring and the 5,7,10(19)-conjugated triene parts, probably because the pocket is tight around these parts. In contrast, the CD ring and side chain part can adopt significantly different conformations, because the pocket around these parts is large and flexible to accommodate structures of various sizes. The latter structural features may be responsible for the potent and differential activities of many agonists having

---

Corresponding Author: Daisuke Morizono

Institute of Biomaterials and Bioengineering, Tokyo Medical and Dental University, 2-3-10 Kanda-Surugadai, Chiyoda-ku, Tokyo 101-0062, Japan

Tel: +81-3-5280-8036 Fax: +81-3-5280-8039

E-mail: daisuke.morizono@teva.jp

Received February 10; Accepted June 10, 2011

modifications at the side chain and/or the CD ring<sup>20</sup>.

Before the VDR crystal structures were clarified, the conformation of vitamin D accommodated in the VDR had attracted much attention, since vitamin D can adopt variable stable conformations because of the flexible 9,10-seco-steroid structure and the full-length cholestane side chain. In solution, the A-ring shows equilibrium of two stable conformations, the  $\alpha$ - and  $\beta$ -chair conformations (Fig.1), as exemplified by NMR studies<sup>21-24</sup>. Okamura et al.<sup>22</sup> successfully predicted that vitamin D would adopt the  $\beta$  conformation at the A-ring when accommodated in the VDR, in which the biologically important 1 $\alpha$ -hydroxyl group has an equatorial conformation. The X-ray crystal structures of VDR-LBD/ligand complexes clearly confirmed that the A-ring invariably adopts the  $\beta$  conformation<sup>14-19</sup>. However, there are still some ambiguities in the structures of the VDR-LBD/vitamin D complexes, since all crystallographic structures filed in the PDB were determined using VDR deletion mutants in which as many as 51 (hVDR) or 47 (rVDR) residues are eliminated from the long loop between helices (H) 1 and 3. The PXR (NR1I2)<sup>25-28</sup>, the phylogenetically nearest (45% sequence identity) neighbor of the VDR, has a similarly long flexible loop between H1 and H3, and this loop 1–3 adopts various conformations so that PXR can bind diverse ligands.

The relationships between side chain conformation and activity was investigated by extensive conformational analysis of active vitamin D derivatives<sup>29-32</sup>. Furthermore, the analysis using <sup>19</sup>F NMR spectroscopy was carried out to probe the conformational change and dynamics of the A-ring and seco-B-ring of vitamin D when vitamin D interacts with the VDR. <sup>19</sup>F NMR has been proven to be a powerful technique for studies of protein structure and dynamics<sup>33,34,53</sup>, because (1) the chemical shift of <sup>19</sup>F is extremely sensitive to changes in the local conformational environment (chemical shift changes as large as 17 ppm have been observed when a <sup>19</sup>F nucleus is incorporated into folded protein); (2) the chemical shift range (~1000 ppm) of the <sup>19</sup>F nucleus is much larger than that of a proton (10 ppm); (3) <sup>19</sup>F does not occur naturally, so there are no background <sup>19</sup>F signals with which to contend; (4) <sup>19</sup>F incorporation is generally nonperturbing to its molecular environment. For this purpose, three fluorinated vitamin D analogs, 4,4-difluoro-1 $\alpha$ ,25-dihydroxyvitamin D<sub>3</sub> [4F<sub>2</sub>-1,25(OH)<sub>2</sub>D<sub>3</sub>, 2]<sup>35</sup> and (10E)- and (10Z)-19-fluoro-1 $\alpha$ ,25-dihydroxyvitamin D<sub>3</sub> [(10E)-19F-1,25(OH)<sub>2</sub>D<sub>3</sub> 3 and (10Z)-19F-1,25(OH)<sub>2</sub>D<sub>3</sub> 4]<sup>36,37</sup> were prepared, and their

spectroscopic as well as biological properties<sup>38</sup> were examined.

In the present study, the <sup>19</sup>F NMR spectra of these fluorinated vitamin D compounds complex with the full-length rat VDR-LBD were measured. By using the geminally fluorinated vitamin D compound 4F<sub>2</sub>-1,25(OH)<sub>2</sub>D<sub>3</sub> (2), the A-ring was shown for the first time to adopt the  $\beta$  conformation in the wild-type receptor in solution. The <sup>19</sup>F signals of the fluorinated vitamin D compounds showed significant chemical-shift changes upon VDR binding. The shielding of <sup>19</sup>F signals using modern *ab initio* molecular orbital (MO) techniques was examined. Herein, the detailed results will be described.

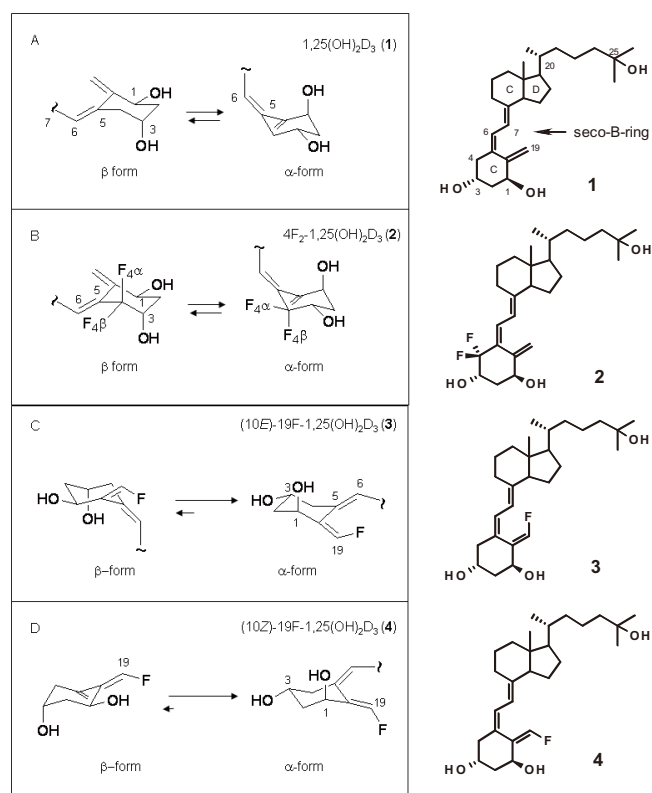


**Figure 1 :** Two A-ring conformations of vitamin D compounds. (A) 1,25(OH)<sub>2</sub>D<sub>3</sub> (1); (B) 4F<sub>2</sub>-1,25(OH)<sub>2</sub>D<sub>3</sub> (2); (C) (10E)-19F-1,25(OH)<sub>2</sub>D<sub>3</sub> (3); and (D) (10Z)-19F-1,25(OH)<sub>2</sub>D<sub>3</sub> (4).

## Materials and Methods

### Expression and purification of rVDR-LBD

Rat VDR-LBD (amino acids 115-423) was expressed as an N-terminal hexahistidine-tagged protein in *E. coli* BL21(DE3)pLysS and purified by a modification of the published procedure<sup>52</sup>. The transformed cells

were plated on a dish (90 mm in diameter) of Luria–Bertani (LB) agar containing ampicillin (100 µg/mL) and chloramphenicol (30 µg/mL), and grown overnight at 37 °C. An isolated colony was inoculated into LB medium (5 mL) supplemented with ampicillin (100 µg/mL) and chloramphenicol (30 µg/mL), and the culture solution was incubated at 37 °C until its OD<sub>600</sub> reached 0.6–0.8. An aliquot (2.5–5 µL) of this pre-culture solution was inoculated into 100 mL of the same LB medium described above and grown similarly at 37 °C for 12 h (OD<sub>600</sub> ~2.4). An aliquot (8.5 mL) of this culture was transferred into 1000 mL of the same LB medium and the cells were grown similarly at 37 °C to an OD<sub>600</sub> of 0.6–0.8 (3–4 h). This culture solution was cooled to 23 °C, isopropyl β-D-thiogalactoside (IPTG) was then added to a final concentration of 12.5 µM to initiate protein expression, and the cells were allowed to grow at 23 °C for 6 h. The cells were harvested by centrifugation (4000 rpm, 20 min, 4 °C) and the pellets were suspended in 10 mL of cell suspension buffer (50 mM NaH<sub>2</sub>PO<sub>4</sub> buffer pH 8.0, 500 mM NaCl, 10 mM imidazole, 1 mM mercaptoethanol). Phenylmethanesulfonyl fluoride (PMSF; 1%) and 1% Tween 20 were added to the suspension and the whole was stored frozen at –80 °C.

The frozen cell suspension (from 1000 mL of culture) was thawed at room temperature and then lysed by sonication (Branson Sonifier 250, VWR, Batavia, IL, USA). The cell lysate was centrifuged at 17000 rpm for 20 min at 6 °C and the supernatant was loaded onto a column of Ni-NTA agarose (2 mL, Qiagen, Santa Clarita, CA, USA), which was pre-equilibrated in the cell suspension buffer. After equilibration for 30 min at room temperature, the column was eluted with 50 mM phosphate buffer (pH 7.5–8.0, 10 mL) containing increasing concentrations of imidazole (20, 50, 100, 150 and 200 mM). The bound protein was then eluted from the resin with phosphate buffer containing 100–200 mM imidazole. Fractions were analyzed by standard SDS-polyacrylamide gel electrophoresis. The fractions containing the desired VDR-LBD protein were collected and dialyzed against 20 mM NaH<sub>2</sub>PO<sub>4</sub> buffer (pH 7.0) containing 5 mM mercaptoethanol, and further purified on a Hi Trap column (Amersham Biosciences Corp., Piscataway NJ, USA). The column was eluted with 20 mM phosphate buffer (pH 7.0, 10 mL) containing increasing concentrations of NaCl (0, 50, 100, and 500 mM): The His-tagged rat VDR-LBD was eluted with the buffer containing 500 mM NaCl. Protein concentration was determined by the Bradford method using BSA as a standard.

### Preparation of NMR samples

Fluorinated vitamin D compounds (2, 3 or 4) (about 2 equivalents of the protein) dissolved in H<sub>2</sub>O (0.5 mL) in the presence of partially methylated 2,3,6-tri-O-methyl-β-cyclodextrin (PMCD, 3 equivalents of the ligand) was added to a solution of VDR-LBD in phosphate buffer obtained in the purification procedure described above. The mixture was allowed to stand overnight at 4 °C and concentrated to about 10% of the original volume by Centriprep-10 (Amicon, Inc., Beverly, MA, USA). To this solution, fresh 20 mM phosphate buffer (pH 7.0, 100 mM NaCl) was added, and the solution was concentrated similarly. These concentration procedures were repeated twice, and finally the protein solution was adjusted to 0.5–1 mM for solution-state NMR or 5–10 mM for solid-state NMR. For solution-state NMR, the protein solution (0.5–1.0 mM, 450 µL) was transferred to a 5-mm NMR tube, which contained a D<sub>2</sub>O solution (50 µL) of a fluorinated vitamin D ligand (1 equivalent of the protein) and PMCD (3 equivalent of the ligand). For solid-state NMR, the protein solution (5–10 mM) containing a ligand (2 equivalents) was poured into a <sup>19</sup>F background-free rotorset (4 mmϕ; JEOL DATUM, Tokyo, Japan).

### FMO calculations

Electron FMO using the ABINIT-MP program (available from <http://www.fsis.iis.u-tokyo.ac.jp/en/results/software/>) at HF/STO-3G level was calculated. In the calculations, proteins were divided into one-residue fragments cutting at the Cα of each residue and treated the ligand as a fragment<sup>40,41</sup>. All calculations were performed on the 27 Xeons GHz network cluster system.

### van der Waals interaction

Van der Waals (vdW) interaction energies were calculated by the MP2 method with Dunning's correlation consistent basis set (aug-cc-pVXZ level)<sup>42,43</sup> on model systems (CH<sub>3</sub>-F for 4F<sub>2</sub>-1,25(OH)<sub>2</sub>D<sub>3</sub>; CH<sub>2</sub>=CF for (10E)-19F-1,25(OH)<sub>2</sub>D<sub>3</sub>; CH<sub>4</sub> for C(δ)H<sub>3</sub> and C(γ)H of Leu; CH<sub>2</sub>=CH<sub>2</sub> for Phe; CH<sub>3</sub>SH for Cys; and CH<sub>3</sub>OH for Ser) where the interacting atoms were overlaid on the positions of the corresponding atoms in the VDR-LBD/fluorinated vitamin D ligand model.

### Model structures

A VDR-LBD/1,25(OH)<sub>2</sub>D<sub>3</sub> (120–423, Δ165–215) model was constructed, in which the structural defects in the crystal structure are amended, from the X-ray crystal structure of human VDR-LBD/1,25(OH)<sub>2</sub>D<sub>3</sub>

complex [PDB code number 1DB1] as described previously<sup>6</sup>. The model structures of three fluorine-substituted vitamin D analogues, (10Z)-19F-1,25(OH)<sub>2</sub>D<sub>3</sub>, (10E)-19F-1,25(OH)<sub>2</sub>D<sub>3</sub>, and 4F<sub>2</sub>-1,25(OH)<sub>2</sub>D<sub>3</sub> and their VDR-LBD complexes were constructed by the following procedure: (i) The natural ligand, 1,25(OH)<sub>2</sub>D<sub>3</sub>, was extracted from the amended VDR-LBD ( $\Delta$ 165–215)/1,25(OH)<sub>2</sub>D<sub>3</sub> complex described above, (ii) a hydrogen at an appropriate position on the ligand was replaced with fluorine, (iii) the modified part, the fluorine and hydrogen on C(19), of the fluorinated vitamin D was refined by optimization at the HF/6-31G level, (iv) the fluorinated vitamin D model constructed at iii was docked into the VDR-LBD model by overlaying with the original ligand 1,25(OH)<sub>2</sub>D<sub>3</sub>, and the MOs of the resulting complex were calculated by the FMO method at the HF/STO-3G level. (v) The VDR-LBD docked with the fluorinated vitamin D was optimized by the molecular mechanics (MM) method under a TRIPOS force field (Tripos, St. Louis), fixing the protein part and the positions of the three hydroxyl groups of the ligand, and the resulting complex was subjected to FMO calculation. (vi) Each fluorinated vitamin D model constructed at iii was fully optimized by *ab initio* MO at the HF/6-31G level to give the free ligand model with optimized geometry. The MO of the resulting free ligand was calculated at the STO-3G level. (vii) The Mulliken populations of the fluorine atoms in all isolated ligands and the ligands in the VDR-LBD were calculated.

## Results

### <sup>19</sup>F NMR studies of fluorinated vitamin D derivatives

The <sup>19</sup>F NMR spectra of the fluorinated vitamin D compounds (2–4) complex with the rat VDR-LBD (amino acids 115–423, no deletion at loop 1–3) were measured. The 4F<sub>2</sub>-1,25(OH)<sub>2</sub>D<sub>3</sub> (2) and 19F-1,25(OH)<sub>2</sub>D<sub>3</sub> isomers (3 and 4) showed different behavior by spectroscopy. The complex of 4F<sub>2</sub>-1,25(OH)<sub>2</sub>D<sub>3</sub> (2) exhibited a clear solution-state <sup>19</sup>F NMR spectrum, but the complexes of (10E)- and (10Z)-19F-1,25(OH)<sub>2</sub>D<sub>3</sub> (3 and 4) did not. For the latter compounds, a magic angle solid-state NMR technique was applied to obtain successfully clear spectra.

#### 4,4-Difluoro-1,25-dihydroxyvitamin D<sub>3</sub> (2)

4F<sub>2</sub>-1,25(OH)<sub>2</sub>D<sub>3</sub> (2) adopts two conformations at the A-ring, the  $\alpha$  and  $\beta$  conformations, in solution as demonstrated by the <sup>19</sup>F and <sup>1</sup>H NMR spectra<sup>38</sup>. At room temperature, this compound exists as an equilibrium mixture of these conformers showing two fluorine

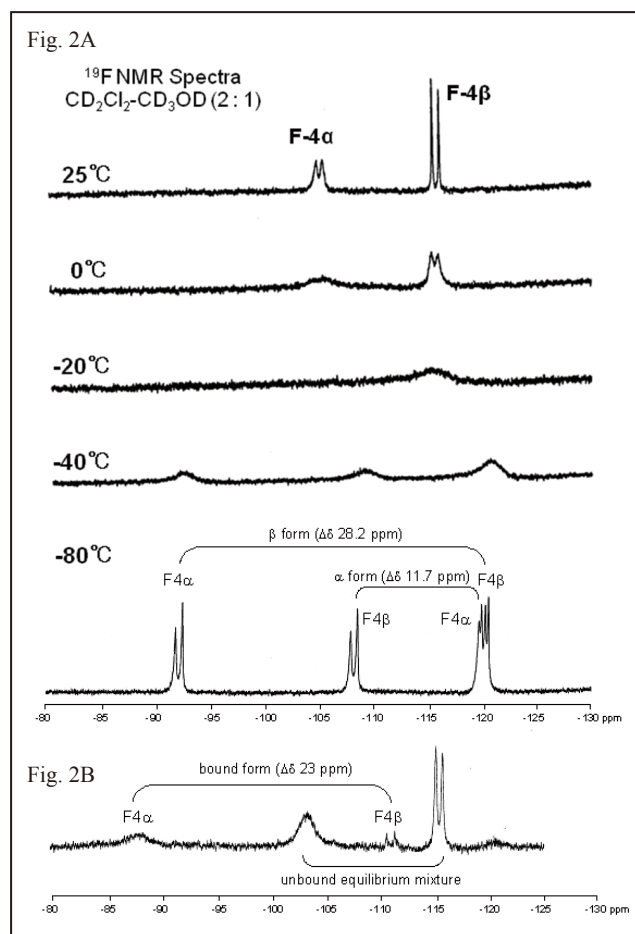


**Figure 2 :** <sup>19</sup>F-NMR spectra of 4F<sub>2</sub>-1,25(OH)<sub>2</sub>D<sub>3</sub> (2)/rVDR-LBD in comparison with the spectra of the free ligands (2). Fig. 2A; The spectrum of free 2 in CD<sub>2</sub>Cl<sub>2</sub>/CD<sub>3</sub>OD (2:1) at 25 °C to -80 °C<sup>38</sup>. Fig. 2B; The spectrum of 4F<sub>2</sub>-1,25(OH)<sub>2</sub>D<sub>3</sub> (2)/rVDR-LBD (AA 116-423) in a phosphate buffer (0.5–1 mM).

signals, -115.1 (F4 $\beta$ ) and -104.5 (F4 $\alpha$ ), as a pair of doublets ( $J = 235$  Hz). The two conformations were observed separately at low temperature (-80 ~ -95 °C): F4 $\alpha$ , -119.9 ( $J = 229$ ,  $\alpha$ -form) & -92.0 ( $J = 241$ ,  $\beta$ -form) and F4 $\beta$ , -108.2 ( $J = 229$ ,  $\alpha$ -form) & -120.2 ( $J = 241$ ,  $\beta$ -form), the ratio of the  $\alpha$  and  $\beta$  conformations being about 1:1 (Fig. 2). The two conformers of 4F<sub>2</sub>-1,25(OH)<sub>2</sub>D<sub>3</sub> (2) are distinct in the <sup>19</sup>F NMR spectra: (1) the signals of F4 $\alpha$  and F4 $\beta$  show greater separation in the  $\beta$  conformer (28.2 ppm) than in the  $\alpha$  conformer (11.7 ppm) (Fig. 2), and (2) the coupling between F4 $\alpha$  and F4 $\beta$  is larger (241 Hz) in the  $\beta$  conformer than in the  $\alpha$  conformer (229 Hz). The signal of the F4 $\alpha$  appears significantly downfield in the  $\beta$  conformer because of the effects of the anti-parallel OH group at C(3) and the  $\pi$  orbitals at C(5,6) that are

**Table 1.** <sup>19</sup>F NMR signal and Mulliken charge of fluorine atoms of three fluorinated vitamin D compounds (2-4).

Compound			<sup>19</sup> F signal ppm (multiplicity, coupling constant Hz)			Mulliken charge <sup>c</sup>		
			free <sup>f</sup>	complex	Δδ	free <sup>f</sup>	complex <sup>g</sup>	Δε
4F <sub>2</sub> -1,25(OH) <sub>2</sub> D <sub>3</sub> (2)	α form	F4α	-119.9 <sup>a</sup> (d, 229)	No <sup>h</sup>		/	/	/
		F4β	-108.2 <sup>a</sup> (d, 229)	No <sup>h</sup>		/	/	/
	β form	F4α	-92.0 <sup>a</sup> (d, 241)	-88 (br <sup>c</sup> )	+4	-0.166	-0.171	-0.005
		F4β	-120.2 <sup>a</sup> (d, 241)	-111 (241 <sup>c</sup> )	+9.2	-0.169	-0.147	+0.021
(10E)-19F-1,25(OH) <sub>2</sub> D <sub>3</sub> (3)	α form	F19	-125.8 <sup>a</sup> (d, 83)	No <sup>h</sup>		/	/	/
	β form	F19	-138.7 <sup>a</sup> (d, 81)	-119 <sup>d</sup>	+19.7	-0.138	-0.131	+0.008
(10Z)-19F-1,25(OH) <sub>2</sub> D <sub>3</sub> (4)	α form	F19	-129.8 <sup>b</sup> (d, 87)	No <sup>h</sup>		/	/	/
	β form	F19	No <sup>h</sup>	-120.5 <sup>d</sup>		-0.145	-0.143	+0.002

The spectra were recorded at -80 ~ -90 °C<sup>a</sup> or at room temperature<sup>b</sup> in CD<sub>2</sub>Cl<sub>2</sub>-CD<sub>3</sub>OD (2:1). The spectra were recorded in phosphate buffer in solution-state<sup>c</sup> or solid-state<sup>d</sup> conditions. <sup>e</sup>The FMO and Mulliken charge were calculated only for the β conformation. <sup>f</sup>Free ligands were fully optimized at HF/6-31G and the Mulliken charges of the optimized ligands were calculated at HF/STO-3G. <sup>g</sup>The ligand to be docked in the VDR-LBD was optimized only around the modified (fluorine substitution) part at HF/6-31G, docked into the VDR-LBD, then optimized by MM method under TRIPOS force field fixing the protein part and the three hydroxyl groups of the ligand, and the FMO of the complex was calculated at HF/STO-3G level. <sup>h</sup>No signal of this conformation was observed in the <sup>19</sup>F NMR spectrum.

nearly parallel to the C4-F4α bond (Fig. 1B): these signals have been assigned on the basis of the <sup>19</sup>F NMR spectra of fluorine-substituted model compounds<sup>38</sup>. This compound (2) was expected to adopt only one of the two conformations when accommodated in the VDR-LBP.

The spectrum of 2 was recorded in 20 mM phosphate buffer containing 0.5–1 mM protein and about 2 molar equivalents of the ligand in the presence of PMCD (3 equivalents of the ligand), which was added to dissolve the ligand in aqueous solvent. Fig. 2 shows a solution-state <sup>19</sup>F NMR spectrum of 4F<sub>2</sub>-1,25(OH)<sub>2</sub>D<sub>3</sub> (2) complex with rVDR-LBD. The <sup>19</sup>F NMR data of fluorinated vitamin D compounds complex with the rVDR-LBD are summarized in Table 1 in comparison with those of the free ligands. The spectrum shows the signals of both free (-115.0 and -103.2 ppm) and VDR-bound 2. The protein-bound 4F<sub>2</sub>-1,25(OH)<sub>2</sub>D<sub>3</sub> (2) showed only a single set of fluorine signals at -88.0 (broad) and -111 ppm (d, *J* = 241 Hz) indicating that it adopts a single conformer. The signal at significantly low field (-88.0 ppm) suggests that F4α adopts an axial conformation with an anti-parallel axial C(3)-OH and π orbitals parallel to the C-F bond. This indicates that the A-ring adopts the β conformation. The significantly large chemical shift difference (23 ppm) between the two fluorine signals and the large coupling constant (241 Hz) also supports the β conformation. It is interesting to note that the signal of F4α appears as broad signal

while F4β exhibits a clear doublet. Probably the axial F4α crowds LBP residues (Fig. 3). Thus, I could demonstrate for the first time, using NMR spectroscopy, that the vitamin D A-ring adopts the β conformation in the wild-type VDR-LBD in solution. In these spectral analyses, the geminal fluorine group was shown to be quite useful on the basis of the chemical shifts and coupling constant.

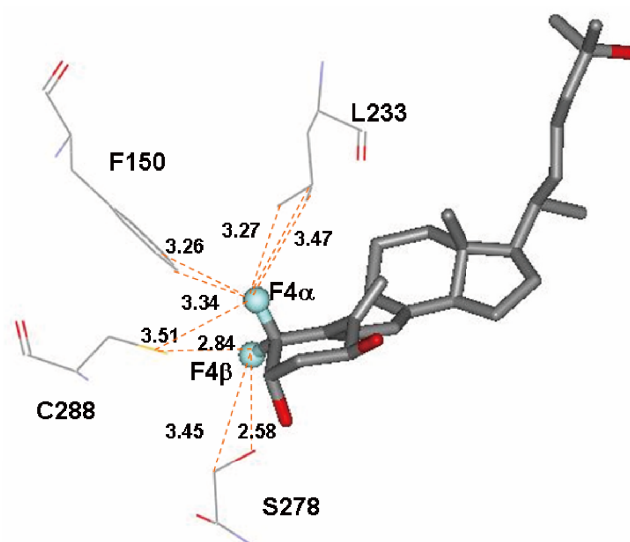


**Figure 3 :** Van der Waals interactions of 4F<sub>2</sub>-1,25(OH)<sub>2</sub>D<sub>3</sub> (2) with LBP residues of the hVDR.

Stick model except for fluorine (ball) with atom-type color. Van der Waals interactions are shown with orange dotted lines.

### (10E)-19-Fluoro-1,25-dihydroxyvitamin D<sub>3</sub> (3)

(10E)-19F-1,25(OH)<sub>2</sub>D<sub>3</sub> (3) is in dynamic equilibrium between the two A-ring conformers, as shown by the <sup>19</sup>F NMR spectrum (84 :16, the  $\alpha$  and  $\beta$  conformers)<sup>38</sup>. It showed a single broad signal ( $\delta$ , -129.6) at room temperature, which was separated into two sharp doublets ( $\delta$ , -125.8,  $J = 83$  Hz and -138.7,  $J = 81$  Hz, 84:16 ratio) at -60 °C. The  $\alpha$  conformer is predominant and appears about 13 ppm downfield from the  $\beta$  conformer. The  $\alpha$  conformer has the axial 1 $\alpha$ -OH group, which would effectively withdraw electron from the 10,19 double bond and have a significant deshielding effect on F(19) (Fig. 4A). The <sup>19</sup>F NMR

spectrum of 3 complex with rVDR-LBD was recorded under conditions similar to those described above for 4F<sub>2</sub> compound 2. However, no clear <sup>19</sup>F signal of protein-bound 3 was observed. The reason for this unclear spectrum in solution-state NMR may be ascribed to the high VDR affinity<sup>38</sup> of (10E)-19F-vitamin D (3), which is 10-folds higher than 2 and 9% of 1,25(OH)<sub>2</sub>D<sub>3</sub> ( $K_d$  10<sup>-11</sup> M<sup>39</sup>). The VDR complex of 3 with the lower dissociation constant would have the longer correlation time ( $\tau_c$ ) and would suffer considerable broadening effects by the dipole moments in comparison to 2.

Thus, a solid-state NMR technique was next applied. The solid-state NMR spectrum of the VDR/3 complex was recorded in a 10-fold more concentrated phosphate buffer solution (5–10 mM) by spinning the sample probe at a rate of 5–15 kHz with the magic angle (54.74°). The spectrum showed two signals at -119 and -128 ppm (Fig. 4A), the former being assigned to the signal of VDR-bound 3 and the latter to the free 3. The signal of the protein-bound 3 appeared 19.7 and 6.8 ppm down-field from those of the free  $\beta$  conformer and the  $\alpha$  conformer, respectively. I assume that protein-bound 3 adopted the  $\beta$  conformation for two reasons: (1) all vitamin D ligands accommodated in the VDR-LBD ( $\Delta$  165–215) are reported to adopt the  $\beta$  conformation without exception, and (2) my data shown above demonstrated that 4F<sub>2</sub>-1,25(OH)<sub>2</sub>D<sub>3</sub> (2) complex with the wild-type rVDR-LBD (no deletion) also adopts the  $\beta$  conformation. The downfield shift (ca. 20 ppm) observed upon protein binding is the largest ever reported for <sup>19</sup>F signals. When accommodated in the LBP, vitamin D ligands are forced to adopt a bent conformation, and F19 crowds with C(7)H and C(18)H<sub>3</sub> in the  $\beta$  conformation (Fig. 5). F19 in the  $\beta$  conformation also crowds L233. These steric perturbations are considered to be the reason for the large chemical shift change, as discussed below.

### (10Z)-19-Fluoro-1 $\alpha$ ,25-dihydroxyvitamin D<sub>3</sub> (4)

Previously, we reported that (10Z)-19F-1,25(OH)<sub>2</sub>D<sub>3</sub> (4) adopts exclusively the  $\alpha$  conformation<sup>38</sup>, because it shows only a single signal at -95 °C as well as at room temperature. Similarly to the *E* isomer 3, (10Z)-19F-1,25(OH)<sub>2</sub>D<sub>3</sub> (4) complex with the rVDR-LBD showed no clear <sup>19</sup>F signal in solution-state NMR. Significant VDR affinity of 4 (8% of that of 1,25(OH)<sub>2</sub>D<sub>3</sub>) was considered to be the reason for this difficulty, as described above for the *E* isomer 3. The solid-state <sup>19</sup>F NMR spectrum of the complex of 4 with VDR-LBD was successfully

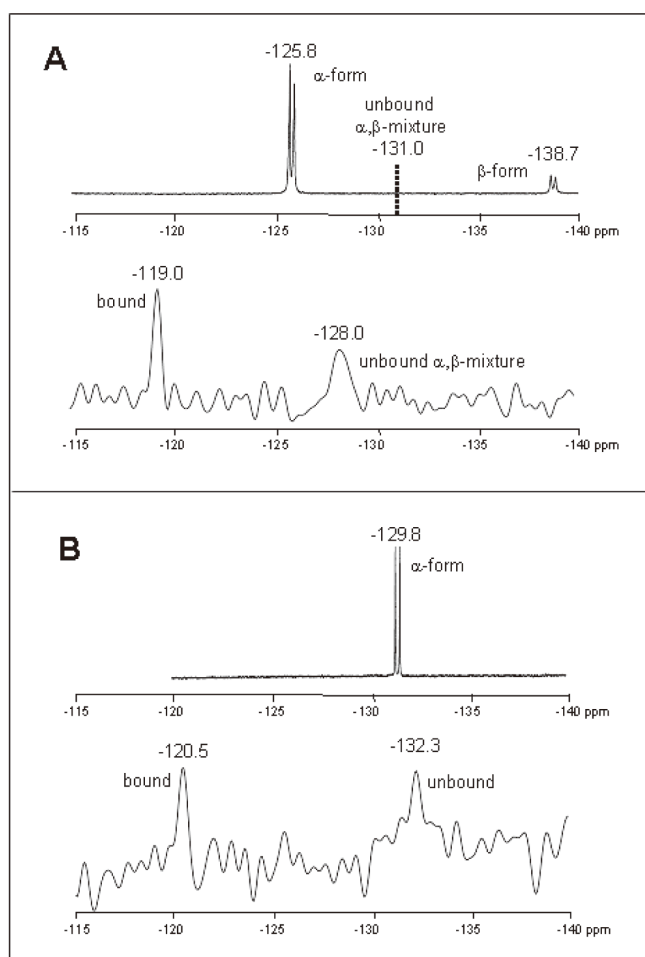


**Figure 4** : Solid-state <sup>19</sup>F-NMR spectra of (10E)- and (10Z)-19F-1,25(OH)<sub>2</sub>D<sub>3</sub> (3 and 4)/rVDR-LBD.

(A) The solid-state spectra of (10E)-19F-1,25(OH)<sub>2</sub>D<sub>3</sub> (3)/rVDR-LBD in phosphate buffer (5–10 mM) (bottom), and the spectrum of free 3 in CD<sub>2</sub>Cl<sub>2</sub>/CD<sub>3</sub>OD (2:1) at -80 °C (top).

(B) The solid state spectrum of (10Z)-19F-1,25(OH)<sub>2</sub>D<sub>3</sub> (4)/rVDR-LBD in phosphate buffer (5–10 mM) (bottom), and the spectrum of free 4 in CD<sub>2</sub>Cl<sub>2</sub>/CD<sub>3</sub>OD (2:1) at room temperature (top).

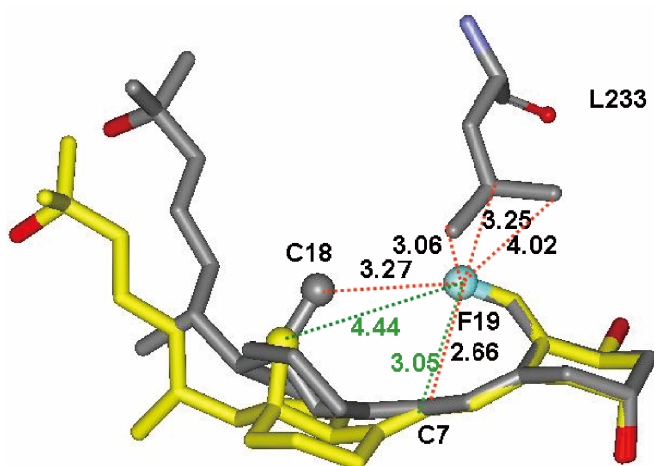


**Figure 5** : Comparison of the conformations of free and VDR-LBD complex (10E)-19F-1,25(OH)<sub>2</sub>D<sub>3</sub> (3).

The models of free (stick model, C yellow, O red and F cyan) and VDR-LBD complex (stick model, atom-type color) (10E)-19F-1,25(OH)<sub>2</sub>D<sub>3</sub> (3) are overlaid. The van der Waals interactions in the free and VDR complex 3 are shown with green and orange dotted lines, respectively.

observed in concentrated phosphate buffer. The NMR spectrum (Fig. 4B) showed two peaks at  $\delta$   $-120.5$  and  $-132.3$ , which are assigned to the signals of the protein-bound and -unbound 4, respectively. The fluorine signal of the free 4 appears upper-field by 2.5 ppm than that observed in organic solvent. The signal of protein-bound 4 appears 11.8 ppm downfield from that of unbound 4 in the  $\alpha$  conformation. The 10Z isomer 4 was also presumed to adopt the  $\beta$  conformation in the LBP for the same reason as the 10E isomer 3. However, there was no further evidence to support this assumption from the present NMR studies.

#### Molecular orbital calculation study

The  $^{19}\text{F}$  chemical shift is extremely sensitive to changes in the local environment<sup>33,34</sup>. A large downfield shift (4–19.7 ppm) of the fluorine signals of compounds 2–4 upon VDR binding was observed. What causes these large changes in the chemical shift? Extensive efforts have been devoted to developing a reliable way of predicting the  $^{19}\text{F}$  shielding effect in terms of molecular structure<sup>43-45</sup>. Four factors are known to contribute to fluorine shielding: (1) local magnetic fields, (2) hydrogen bond formation, (3) electrostatic fields from dipoles or formal charges, and (4) vdW interactions.

When a ligand is incorporated into the narrow LBP of

the receptor, it is forced into contact with numerous amino acid residues, experiencing intense vdW interactions. In fact the vdW interactions in addition to electrostatic field effects have been shown to play an important role in the shielding of fluorine signals<sup>33,34,44-46</sup>. *Ab initio* MO methods were applied to explain the large chemical shift changes of the fluorine signals of the ligand that occur upon VDR binding. The fragment MO (FMO) method (Hartree-Fock (HF)/STO-3G level)<sup>40,41</sup> was examined for calculating the factors 1–3 above and the second order Moller–Plesset method (MP2) with Dunning’s correlation consistent basis set (aug-cc-pVXZ level)<sup>42,43</sup> for factor 4. The FMO method is an *ab initio* MO method developed recently for biological macromolecules where a large molecule is divided into fragments and the MOs of the fragments and fragment pairs are calculated. It is generally accepted that chemical shifts are closely related to gross atomic charges<sup>47</sup>, but atomic charge distribution is difficult to calculate correctly due to its high dependency on basis set functions<sup>48</sup>. Several methods have been developed to avoid this problem<sup>49</sup>. However, Mulliken population analysis was used, because it affords information on a traditional orbital basis and it seemed to be appropriate for the present purpose. Since the FMO method excludes the electron correlation term, the vdW energies by the MP2 method was calculated. Because of the limitation of the MP2 method in applying macromolecules, the vdW energies on simple model systems with counter poise correction was calculated<sup>50</sup>. Thus, models of fluorinated vitamin D compounds (2–4) complex with hVDR-LBD were prepared by modifying the crystal structure (1DB1) of hVDR-LBD complex with 1,25(OH)<sub>2</sub>D<sub>3</sub><sup>51</sup>. The MOs of the free fluorinated vitamin D ligands (2–4) were calculated by the *ab initio* MO method (HF/STO-3G) whereby they were fully optimized. The results of the calculation are shown in Tables 1 and 2.

**4F<sub>2</sub>-1,25(OH)<sub>2</sub>D<sub>3</sub> (2)**. It is generally accepted that the chemical shifts and electron density are correlated. The Mulliken charges of 4F $\alpha$  ( $-0.166$ ) and 4F $\beta$  ( $-0.169$ ) of 2 are barely correlated with their  $^{19}\text{F}$  chemical shifts (Table 1). However, in the protein complex, the charges of fluorine atoms are hardly correlated with their chemical shifts. In the present study, it was revealed that, upon complex formation, both the electron charge and vdW interaction had a similar effect on the shielding of the fluorine atoms. The F4 $\alpha$  signal shifts downfield (+4 ppm), in contrast with the slight increment of the electron density ( $-0.005$ ). F4 $\alpha$  interacts with Leu233, Phe150 and Cys288, and has significant vdW energies

**Table 2.** Van der Waals interactions of F atom of VDR ligands in the VDR complex

Compound	Interacting group of atoms <sup>a</sup>		Distance (Å) <sup>c</sup>	Interaction energy <sup>d</sup> (kcal/mol)	
		model <sup>b</sup>			
4F <sub>2</sub> -1,25(OH) <sub>2</sub> D <sub>3</sub> (2)	F4α	<b>L233</b>			
		C(δ1)H <sub>3</sub>	CH <sub>4</sub>	3.27	-0.638
		C(δ2)H <sub>3</sub>	CH <sub>4</sub>	3.47	-0.508
		<b>F150</b>			
		C(3)HC(4)H	CH <sub>2</sub> =CH <sub>2</sub>	3.26, 3.34	-0.835
	<b>C288</b>				
	Sγ	CH <sub>3</sub> SH	3.51	-0.964	
	total			-2.945	
	F4β	<b>S278</b>			
		C(β)H <sub>2</sub> ,Oγ	CH <sub>3</sub> OH	3.45, 2.58	-1.344
<b>C288</b>					
Sγ		CH <sub>3</sub> SH	2.84	-1.473	
total				-2.816	
(10E)-19F-1,25(OH) <sub>2</sub> D <sub>3</sub> (3)	<b>L233</b>				
	C(δ1)H <sub>3</sub>	CH <sub>4</sub>	4.02	-0.725	
	C(δ2)H <sub>3</sub>	CH <sub>4</sub>	3.06	-1.016	
	C(γ)H	CH <sub>4</sub>	3.25	-0.993	
	<b>Intra</b>				
	C(18)H <sub>3</sub>	CH <sub>4</sub>	3.27	-0.531	
	C(8)=C(7)H	CH <sub>2</sub> =CH <sub>2</sub>	2.66	-0.914	
	Total			-4.179	

<sup>a</sup>Group of atoms that have van der Waals contact with the F atoms of the ligands (4.1 Å cut off): Some intramolecular interactions that had significant change upon complex formation are included. <sup>b</sup>Van der Waals interaction energies are calculated using model systems. <sup>c</sup>Distance between non-hydrogen atoms. <sup>d</sup>The MOs and energies of three systems (ligand, residues, and ligand/residue complex) were calculated on the models by *ab initio* MP2 method (Dunning's correlation consistent basis set, aug-cc-pVXZ [42,43]). The van der Waals interaction energies ( $\Delta E$ ) were obtained by the following:  $\Delta E = E_{\text{complex}} - (E_{\text{residue}} + E_{\text{ligand}})$ .

between these residues (-2.945 kcal/mol in total), which would shift the signal significantly downfield. Thus, combination of the Mulliken charge and vdW energy can reasonably explain the chemical shift change in the F4α signals. F4β interacts with Cys288 and Ser278 and also has a similarly large (-2.816 kcal/mol) total vdW energy. This, together with a decrease of the Mulliken charge (+0.021), explains the large chemical shift change (+9.2 ppm).

(10E)-19F-1,25-(OH)<sub>2</sub>D<sub>3</sub> (3). The F19 signal of 3 experiences a large chemical shift change (19.7 ppm) upon VDR binding, the largest chemical shift change ever observed when a <sup>19</sup>F nucleus is incorporated into a folded protein. The slight decrease of the Mulliken charge of 3 (+0.008) cannot explain this large downfield shift. The F19 has only Leu233 in close proximity. Therefore the reason was assumed to be the

intramolecular vdW interaction due to steric congestion of F19 with C(7)H and C(18)H<sub>3</sub> in the complex. Vitamin D ligands are forced to adopt a bent conformation when incorporated into the LBP. In the bent conformation, F19 crowds C(18)H<sub>3</sub> and C(7) (Fig. 5). As expected, the intramolecular vdW energies of F19 with C(18)H<sub>3</sub> and C(7)H increased (-1.445) significantly when the ligand adopted a bent conformation. The intramolecular interaction of F19 with CH<sub>3</sub>(18) occurs only when it adopts the β conformation.

## Discussion

In this paper, the <sup>19</sup>F NMR spectra of the complex of the fluorinated vitamin D derivatives with the full-length rat VDR-LBD were examined in detail. The two observed conformers of 4F<sub>2</sub>-1,25(OH)<sub>2</sub>D<sub>3</sub> (2) was assigned to the

known  $\alpha$  and  $\beta$  conformers formed by the flipping of the A-ring. The single conformation observed for (10Z)-19F-1,25(OH)<sub>2</sub>D<sub>3</sub> (4) was assigned to the  $\alpha$  conformer. On the other hand, the <sup>19</sup>F NMR spectra of the complex of the fluorinated vitamin D derivatives with the full-length rat VDR-LBD showed that the A-ring adopts the  $\beta$  conformation in the wild-type receptor in solution. This biological information in combination with the NMR properties indicates that the fluorinated vitamin D derivatives are promising probes for studying the VDR-bound A-ring conformation of vitamin D.

### Acknowledgements

I wish to thank Sachiko Yamada (School of Medicine, Nihon University) and Masato Shimizu (Institute of Biomaterials and Bioengineering, Tokyo Medical and Dental University).

### References

- Evans, R.M. (1988). The Steroid and Thyroid Hormone Receptor Superfamily. *Science* 240, 889-895.
- Mangelsdorf, D.J., Thummel, C., Beato, M.; Herrlich, P., et al. (1995). The Nuclear Receptor Superfamily: the Second Decade. *Cell* 83, 835-839.
- Chambon P. (1996). A decade of molecular biology of retinoic acid receptors. *FASEB J.* 10, 940-954.
- Shulman, A.I., Larson, C., Mangelsdorf, D.J., et al. (2004). Structural Determinants of Allosteric Ligand Activation in RXR Heterodimers. *Cell* 116, 417-429.
- Lockless, S.W. and Ranganathan, R. (1999). Evolutionally conserved pathways of energetic connectivity in protein families. *Science* 286, 295-299.
- Yamamoto, K., Abe, D., Yoshimoto, N., et al. (2006). Vitamin D Receptor: Ligand Recognition and Allosteric Network. *J. Med. Chem.* 49, 1313-1324.
- Yamada, S. and Yamamoto, K. (2006). Ligand recognition by vitamin D receptor: total alanine scanning mutational analysis of the residues lining the ligand binding pocket of vitamin D receptor. *Curr. Top. Med. Chem.* 6, 1255-1265.
- Bourguet, W., Ruff, M., Chambon, P., et al. (1995). Crystal Structure of the Ligand-Binding Domain of the Human Nuclear Receptor RXR- $\alpha$ . *Nature* 375, 377-382.
- Renaud, J.-P., Rochel, N., Ruff, M., et al. (1995). Crystal Structure of the RAR- $\gamma$  Ligand-Binding Domain Bound to All-*Trans* Retinoic Acid. *Nature* 378, 681-689.
- Brzozowski, A.M., Pike, A.C., Dauter, Z., et al. (1997). Molecular Basis of Agonism and Antagonism in the Oestrogen Receptor. *Nature* 389, 753-758.
- Xu, H.E., Stanley, T.B., Montana, V.G., et al. (2002). Structural Basis for Antagonist-Mediated Recruitment of Nuclear Co-repressors by PPAR $\alpha$ . *Nature* 415, 813-817.
- Shiau, A.K., Barstad, D., Loria, P.M., et al. (1998). The Structural Basis of Estrogen Receptor/Coactivator Recognition and the Antagonism of This Interaction by Tamoxifen. *Cell* 95, 927-937.
- Greschik, H. and Moras, D. (2003). Structure-activity relationship of nuclear receptor-ligand interactions. *Curr. Top. Med. Chem.* 3, 1573-1599.
- Rochel, N., Wurtz, J.M., Mitschler, A., et al. (2000). The Crystal Structure of the Nuclear Receptor for Vitamin D Bound to Its Natural Ligand. *Mol. Cell* 5, 173-179.
- Tocchini-Valentini, G., Rochel, N., Wurtz, J.M., et al. (2001). Crystal structures of the vitamin D receptor complex to super agonist 20-epi ligands. *Proc. Natl. Acad. Sci. USA* 98, 5491-5496.
- Tocchini-Valentini, G., Rochel, N., Wurtz, J.-M., et al. (2004). Crystal Structures of the Vitamin D Nuclear Receptor Liganded with the Vitamin D Side Chain Analogues Calcipotriol and Seocalcitol, Receptor Agonists of Clinical Importance. Insights into a Structural Basis for the Switching of Calcipotriol to a Receptor Antagonist by Further Side Chain Modification. *J. Med. Chem.* 47, 1956-1961.
- Vanhook, J.L., Benning, M.M., Bauer, C.B., et al. (2004). Molecular Structure of the Rat Vitamin D Receptor Ligand Binding Domain Complex with 2-Carbon-Substituted Vitamin D<sub>3</sub> Hormone Analogues and a LXXLL-Containing Coactivator Peptide. *Biochemistry* 43, 4101-4110.
- Eelen, G., Verlinden, L., Rochel, N., et al. (2005). Superagonistic Action of 14-Epi-Analogs of 1,25-Dihydroxyvitamin D Explained by Vitamin D Receptor-Coactivator Interaction. *Mol. Pharmacol.* 67, 1566-1573.
- Hourai, S., Fujishima, T., Kittaka, A., et al. (2006). Probing a water channel near the A-ring of receptor-bound 1 $\alpha$ ,25-dihydroxyvitamin D<sub>3</sub> with selected 2 $\alpha$ -substituted analogues. *J. Med. Chem.* 49, 5199-5205.
- Yamada, S., Shimizu, M. and Yamamoto, K. (2003). Structure-function relationships of vitamin D including ligand recognition by the vitamin D receptor. *Med. Res. Rev.* 23, 89-115.
- La Mar, G.N. and Budd, D.L. (1974). Elucidation of the Solution Conformation of the A Ring in Vitamin D Using Proton Coupling Constants and a Shift Reagent. *J. Am. Chem. Soc.* 96, 7317-7324.
- Wing, R.M., Okamura, W.H., Rego, A., et al. (1974). Vitamin D in Solution: Conformations of Vitamin D<sub>3</sub>, 1 $\alpha$ ,25-Dihydroxyvitamin D<sub>3</sub>, and Dihydrotachysterol<sub>3</sub>. *Science* 186, 939-941.
- Wing, R.M., Okamura, W.H., Rego, A., et al. (1975). Studies on Vitamin D and Its Analogs. VII. Solution Conformations of Vitamin D<sub>3</sub> and 1 $\alpha$ ,25-Dihydroxyvitamin D<sub>3</sub> by High-Resolution Proton Magnetic Resonance Spectroscopy. *J. Am. Chem. Soc.* 97, 4980-4985.
- Eguchi, T. and Ikekawa, N. (1990). Conformational Analysis of 1 $\alpha$ ,25-Dihydroxyvitamin D<sub>3</sub> by Nuclear Magnetic Resonance. *Bioorg. Chem.* 18, 19-29.
- Watkins, R.E., Wisely, G.B., Moore, L.B., et al. (2001). The human nuclear xenobiotic receptor PXR: structural determinants of directed promiscuity. *Science* 292,

- 2329-2333.
26. Chrencik, J.E., Orans, J.O., Moore, L.B., et al. (2003). Structural disorder in the complex of human pregnane x receptor and the macrolide antibiotic rifampicin. *Mol. Endocrinol.* 19, 1125-1134.
  27. Watkins, R.E., Maglich, J.M., Moore, L.B., et al. (2003). 2.1 A Crystal Structure of Human PXR in Complex with the St. John's Wort Compound Hyperforin. *Biochemistry* 42, 1430-1438.
  28. Chrencik, J.E., Orans, J.O., Moore, L.B., et al. (2005). Structural disorder in the complex of human pregnane x receptor and the macrolide antibiotic rifampicin. *Mol. Endocrinol.* 19, 1125-1134.
  29. Yamamoto, K., Ohta, M., DeLuca, H.F., et al. (1995). On the side chain conformation of 1 $\alpha$ , 25-dihydroxyvitamin D<sub>3</sub> responsible for binding to the receptor. *Bioorg. Med. Chem. Lett.* 5, 979-984.
  30. Yamamoto, K., Sun, W-Y., Ohta, M., et al. (1996). Conformationally restricted analogs of 1 $\alpha$ , 25-dihydroxyvitamin D<sub>3</sub> and its 20-epimer: Compounds for study of the three-dimensional structure of vitamin D responsible for binding to the receptor. *J. Med. Chem.* 39, 2727-2737.
  31. Yamada, S., Yamamoto, K., Masuno, H., et al. (1998). Conformation-function relationship of vitamin D: Conformational analysis predicts potential side chain structure. *J. Med. Chem.* 41, 1467-1475.
  32. Yamamoto, K., Ooizumi, H., Umesono, K., et al. (1999). Three-dimensional structure-function relationship of vitamin D: side chain location and various activities. *Bioorg. Med. Chem. Lett.* 1041-1046.
  33. Danielson, M.A. and Falke, J.J. (1996). Use of <sup>19</sup>F NMR to probe protein structure and conformational changes. *Annu. Rev. Biophys. Biomol. Struct.* 25, 163-195.
  34. Gerig, J.T. (1994). Fluorine NMR of proteins. *Progress in NMR Spectroscopy*, 26, 293-370.
  35. Shimizu, M., Iwasaki, Y. and Yamada, S. (1999). 4, 4-Difluoro-1 $\alpha$ ,25-dihydroxyvitamin D<sub>3</sub>: Analog to probe A-ring conformation in vitamin D-receptor complex. *Tetrahedron Lett.* 40, 1697-1700.
  36. Shimizu, M., Iwasaki, Y., Ohno, A., et al. (2000). (10Z)- and (10E)-19-Fluoro-1 $\alpha$ ,25-dihydroxyvitamin D<sub>3</sub>: compounds to probe vitamin D conformation in receptor complex by <sup>19</sup>F-NMR. *Chem. Pharm. Bull.* 48, 1484-1493.
  37. Shimizu, M., Ohno, A. and Yamada, S. (2001). (10Z)- and (10E)-19-Fluoro-1 $\alpha$ ,25-dihydroxyvitamin D<sub>3</sub>: an improved synthesis via 19-nor-10-oxo-vitamin D. *Chem. Pharm. Bull.* 49, 312-317.
  38. Ohno, A., Shimizu, M. and Yamada, S. (2002). Fluorinated vitamin D analogs to probe the conformation of vitamin D in its receptor complex: <sup>19</sup>F NMR studies and biological activity. *Chem. Pharm. Bull.* 50, 475-483.
  39. Haussler, M.R., (1986). Vitamin D receptors: nature and function. 6, 527-562.
  40. Kitaura, K., Ikeo, E., Asada, T., et al. (1999). Fragment molecular orbital method: an approximate computational method for large molecule. *Chem. Phys. Lett.* 313, 701-706.
  41. Nakano, T., Kaminuma, T., Sato, T., et al. (2000). Fragment molecular orbital method; application to polypeptides. *Chem. Phys. Lett.* 318, 614-618.
  42. Tsuzuki, S., Uchimaru, T., Mikami, M., et al. (2003). Ab initio calculation of intermolecular interaction of CHF<sub>3</sub> dimer: Origin of attraction and magnitude of CH/F interaction. *J. Phys. Chem. A* 107, 7962-7968.
  43. Kryachko, E. and Scheiner, S. (2004). CH...F Hydrogen bonds. Dimers of fluoromethanes. *J. Phys. Chem. A* 108, 2527-2535.
  44. de Dios, A.C., Pearson, J.G. and Oldfield E. (1993). Secondary and tertiary structural effects on protein NMR chemical shifts: an ab initio approach. *Science* 260, 1491-1496.
  45. Pearson, J.G., Oldfield, E., Lee, F.S., et al. (1993). Chemical shifts in proteins: a shielding trajectory analysis of the fluorine nuclear magnetic resonance spectrum of the Escherichia coli galactose binding protein using a multipole shielding polarizability-local reaction field-molecular dynamics approach. *J. Am. Chem. Soc.* 115, 6851-6862.
  46. Chambers, S.E. Lau, E.Y. and Gerig, J.T. (1994). Origins of Fluorine Chemical Shifts in Proteins. *J. Am. Chem. Soc.* 116, 3603-3604.
  47. Fukuda, R. and Nakatsuji, H. (2005). Atomic charges based on spherical harmonics expansion at the atomic centers. *J. Chem. Phys.* 123; Art No.044101.
  48. Monaco, G. (1998). On the definition of the atomic charge. Relationship between <sup>13</sup>C NMR chemical shifts, dipole moments, and charges in saturated hydrocarbons. *Int. J. Quant. Chem.* 68, 201-210.
  49. Larsson, S. and Braga, M. (1985). Atomic charges based on spherical harmonics expansion at the atomic centers. *Theor. Chim. Acta* 68, 291-300.
  50. Simon, S. M., Duran, M. J. J., Dannenberg, J. J. (1996). How does basis set superposition error change the potential surfaces for hydrogen-bonded dimers? *J. Chem. Phys.* 105, 11024-11031.
  51. Verboven, C., Rabijns, A., De Maeyer, M., et al. (2002). A structural basis for the unique binding features of the human vitamin D-binding protein. *Nat. Struct. Biol.* 9, 131-136.
  52. Strugnelli, S.A., Hill, J.J., McCaslin, D.R., et al. (1999). Bacterial expression and characterization of the ligand-binding domain of the vitamin D receptor. *Arch Biochem Biophys* 364, 42-52.
  53. Cory, D.G. and Ritchey, W. M. (1988). Suppression of signals from the probe in block decay spectra. *J Magn Reson* 80, 128-132.